

Growth of individual carbon nanotubes on an array of TiN/Ni nanodots patterned by e-beam lithography and defined by dry etching for field emission application

Xiang-Lei Han, Jean-Paul Mazellier, Laurent Gangloff, Florian Andrianiazy, Zhenkun Chen, Costel Sorin Cojocaru, Jean-Luc Maurice, Emilien Peytavit, Jean-Francois Lampin, Pierre Legagneux

▶ **To cite this version:**

Xiang-Lei Han, Jean-Paul Mazellier, Laurent Gangloff, Florian Andrianiazy, Zhenkun Chen, et al.. Growth of individual carbon nanotubes on an array of TiN/Ni nanodots patterned by e-beam lithography and defined by dry etching for field emission application. 2013. hal-00880711

HAL Id: hal-00880711

https://polytechnique.hal.science/hal-00880711

Preprint submitted on 8 Feb 2014

HAL is a multi-disciplinary open access archive for the deposit and dissemination of scientific research documents, whether they are published or not. The documents may come from teaching and research institutions in France or abroad, or from public or private research centers.

L'archive ouverte pluridisciplinaire **HAL**, est destinée au dépôt et à la diffusion de documents scientifiques de niveau recherche, publiés ou non, émanant des établissements d'enseignement et de recherche français ou étrangers, des laboratoires publics ou privés.

Growth of individual carbon nanotubes on an array of TiN/Ni nanodots patterned by e-beam lithography and defined by dry etching for field emission application.

Xiang-Lei Han [a, *], Jean-Paul Mazellier [b], Laurent Gangloff [b], Florian Andrianiazy [b], ZhenKun Chen [a], Costel Sorin Cojocaru [c], Jean-Luc Maurice [c], Emilien Peytavit [a], Jean-François Lampin [a] and Pierre Legagneux [b]

a). IEMN/UMR CNRS 8520, Avenue Poincaré, BP 60069, 59652 Villeneuve d'Ascq Cedex, France
b). Nanocarb, Thales Research and Technology, 1 Av. Augustin Fresnel 91767 Palaiseau, France
c). LPICM/UMR CNRS 7647, Ecole Polytechnique, Route de Saclay, 91128 Palaiseau Cedex, France

* xianglei.han@isen.iemn.univ-lille1.fr

Keywords:

Individual vertically aligned carbon nanotubes, Electron-beam lithography, Dry etching, Field emission

Abstract:

In this paper, we demonstrate a new technique to realize TiN/Ni nanodots array on silicon substrate using e-beam lithography and dry etching techniques. After patterning the Ni nanodisk (7 nm thick, 150 nm in diameter) at perfectly controlled location, individual vertically aligned carbon nanotubes (VACNTs) were grown using plasma-enhanced chemical-vapor deposition (PECVD). In addition, a field emission cathode (1 mm diameter circular emission area) based on a hexagonal array (20μm spacing) of individual VACNTs delivered a high emission current of 4.23 mA for an applied electric field of 22.5V/μm.

Introduction

Carbon nanotubes (CNTs) are recognized to have high potential for applications in many fields such as nanoelectronic devices [1-3] or field-emission sources [4-9], because of their nanometer scale size, high aspect ratio and remarkable electrical properties. In order to achieve good and uniform electronic emission, cathodes based on vertically aligned carbon nanotubes (VACNTs) are patterned as an array with a pitch defined as twice the VACNTs height to avoid electrical field screening [7, 8]. Individual CNTs can be precisely grown on Ni catalyst nanodisks realized by combining e-beam [9, 10] or nanoimprint lithography [11] with lift-off. After realizing holes in a resin layer, a TiN film (acting as a diffusion barrier) is deposited by sputtering and a Ni layer is evaporated. This method allows growing regular arrays of VACNTs but lacks of reliability and reproducibility because the lift-off process is critical in particular for sputtered layers. Moreover, the deposited TiN film contains carbon and oxygen species probably originating from resist outgasing during sputtering. In order to realize uniform array of individual VACNTs, it is necessary to develop a new technology to fabricate the Ni catalyst nanodisks with a high control on their dimension and location.

Ni nanodisk array fabrication

The fabrication process used in this work is described schematically in Figure 1. After depositing bi-layer of TiN/Ni, Hydrogen SilsesQuioxane (HSQ) nanopillars array was patterned by e-beam lithography. Subsequently, the dry etching was employed to etch

Ni and TiN layers. Following the stripping of HSQ resist, the Ni nanodisks array was realized and the individual VACNTs have been grown.

Initially, a 2 inches n-type doped Si (100) substrate was cleaned in acetone during 5 min and rinsed in isopropanol (IPA) during 1 min to remove organic contamination. Then the native oxide present on the Si substrate was etched in a 1% HF solution during 1 min. A 15 nm thick TiN diffusion barrier and a 7 nm thick Ni film were subsequently deposited on the Si substrate by magnetron sputtering (ALLIANCE Concept DP650) and electron-beam evaporation (PLASSYS MEB 550S) respectively. This has been controlled by cross-section observation using a high resolution of scanning electron microscope (HRSEM, a ZEISS Ultra 55) as shown in Figure 2 . A well-defined array of HSQ nanodots has been patterned by e-beam lithography (VISTEC 5000+) using a high acceleration voltage (100 kV) and a small electrons beam current (1 nA). HSQ resist has been developed in a concentrated developer solution (25 % TMAH) during 1 min, rinsed in deionized water and blown dry by nitrogen. We can notice that HSQ nanopilars exhibited a high contrast value (see ref [12]). Figure 3 shows that the HSQ resist patterns on Ni surface was obtained with 134 nm diameter, 82 nm height the patterns were then transferred by IBE with 300 eV ions energy, 500 W power and 5.3 A current (PLASSYS MU350) for etching the 7 nm thick Ni layer. However, during IBE, the sputtered Ni atoms tend to redeposit on the HSQ nanopillars (Ni film thickness around 7 nm). This generated the HSQ/Ni core/shell structures shown in Figure 4 (a). The diameter of mask becomes larger to nearly 150 nm. Reactive ion etching (RIE) was employed to etch the 15 nm thick TiN layer using plasma Cl_2 with Ar ion-assisted

physical bombardment, under a plasma power of 150 W and a pressure as low as 3 mTorr (OXFORD Plasmalab System100) [13]. As shown in Figure 4 (b), the silicon substrate was also partially etched. Lastly, the HSQ nanopillars were stripped in a "Padetch" solution (NH_4F: $C_2H_4O_2$) and rinsed in deionized water. Figure 4 (c) HRSEM image shows the Si/TiN/Ni nanopilars array. The magnified HRSEM image on Figure 4 (d) shows that the Ni nanodisks exhibit no significant imperfections. Final dimensions of the nanopilars, as measured by 30° tilt HRSEM observation, is 150 nm in diameter on the whole stack, thicknesses are 7 nm for Ni, 15 nm thickness for TiN and 50 nm for etched Si (see inset in Figure 4). We can notice these dimensions meet exactly the targeted values. Such Ni nanodisk allows the growth of individual VACNT [9].

Growth of individual VACNT array and field emission characterization

After realization of Ni nanodisk arrays, individual VACNTs array was grown in plasma enhanced chemical vapor deposition (PECVD) reactor using a mixture of C_2H_2 and NH_3 (1:3.5) at 6 mbar, at 750°C for 10 min. This process allows producing straight VACNTs, as shown on Figure 5. VACNTs length is about 5 μm and pitch is 20 μm as defined by Ni catalyst nanodisks patterning previously described. In addition, it is noted that at each array node stands an individual VACNT. On the whole emission area (1mm in diameter) a highly uniform length distribution has been observed. This demonstrates that our new process of Ni nanodisks is well controlled and highly uniform and reproducible as well as the VACNTs growth process.

After growth of VACNTs array, an annealing process (900°C for 1 hour in vacuum) is realized to enhance emission performances. Subsequently, field emission measurements have been performed. As illustrated by Figure 6, VACNTs cathode is placed in front of an extraction grid, both elements being separated by a SiO_2 spacer (40µm thick) which allows precise and constant cathode-grid distance during field emission. Cathode is negatively polarized to high voltage in DC mode during measurement. An anode is placed in front of the setup in order to collect electrons that are not intercepted by the grid. It also ensures that measured current is not due to parasitic effect (such a spacer wall leakages).

We measured a field emission current up to 4.23 mA, which represents a current density of 0.54 A/cm², at extraction voltage of 22.5 V/µm. We can notice here that the array pitch is 20 µm, twice the minimum pitch required (10 µm for VACNTs 5µm long) to avoid electrostatic screening between adjacent VACNTs.

Conclusion

In this work, we successfully developed a new method combining e-beam lithography and dry etching to realize Ni nanodisks with 7 nm of thickness and 150 nm of diameter array. Highly uniform arrays of individual and VACNTs were grown by PECVD with a perfect control of their location on the Si substrate. A 1 mm diameter large hexagonal array of VACNTs (20 µm pitch) delivered a high emission current of 4.23 mA for an applied electric field of 22.5V/µm. By combining this individual VACNTs array with photodetectors array [14], we aim to optically control the emitted current.

Acknowledgement

This work was financially supported by the French National Research Agency National Programme (ANR – NANOSCANNER) and French RENATECH network (French National Nanofabrication Platform).

References:

[1] Sander J. Tans, Alwin R. M. Verschueren and Cees Dekker, *Nature,* Vol. 393, (1998) p. 49-52

[2] K.B.K. Teo, E. Minoux, L. Hudanski, F. Peauger, J-P. Schnell, L. Gangloff, P. Legagneux, D. Dieumegard, G.A.J. Amaratunga, W.I. Milne, *Nature,* Vol. 437, No. 13, (2005), p. 968

[3] A. Bachtold, P. Hadley, T. Nakanishi, C. Dekker, *Science,* Vol. 294 no. 5545 (1999), p. 1317-1320

[4] E. Minoux, O. Gröning, K. B. K. Teo, S. H. Dalal, L. Gangloff, J. P. Schnell, L. Hudanski, I. Y. Y. Bu, P. Vincent, P. Legagneux, G. A. J. Amaratunga, and W. I. Milne, *Nano Lett*. Vol. 5, No. 11, (2005), p. 2135-2138

[5] G Pirio, P Legagneux, D Pribat, K B K Teo, M Chhowalla, G A J Amaratunga and W I Milne, *Nanotechnology*, Vol. 13 No. 2, (2002), p. 1-4

[6] S. Fan, Michael G. Chapline, N. R. Franklin, T. W. Tombler, Alan M. Cassell and H. Dai, *Science,* Vol. 283 no. 5401 (1999) p. 512-514

[7] L. Nilsson, O. Groening, C. Emmenegger, O. Kuettel, E. Schaller, L. Schlapbach, H. Kind,J.M. Bonard and K. Kern, *Appl. Phys. Lett.* Vol. 76, No. 15, (2000), p. 2071

[8] J. M. Bonard, N. Weiss, H. Kind, T. Stockli, L. Forro, K. Kern, and A. Chatelain, *Adv. Mater*. Vol. 13, (2001), p. 184

[9] K.B.K. Teo, S-B. Lee, M. Chhowalla, V Semet, V.T. Binh, O. Groening, M. Castignolles, A. Loiseau, G. Pirio, P. Legagneux, D. Pribat, D. G. Hasko, H. Ahmed, G.A.J. Amaratunga and W.I. Milne, *Nanotechnology*, Vol. 14, No. 2, (2003), p. 204-211.

[10] L.Gangloff, E. Minoux, K. B. K. Teo, P. Vincent, V. T. Semet, V. T. Binh, M. H. Yang, I. Y. Y. Bu, R. G. Lacerda, G. Pirio, J. P. Schnell, D. Pribat, D. G. Hasko, G. A. J. Amaratunga, W. I. Milne and P. Legagneux, *Nano Lett*. Vol. 4, No. 9, (2005), p. 1575-1579

[11] Sara M. C. Vieira, Kenneth B. K. Teo, William I. Milne, Oliver Gröning, Laurent Gangloff, Eric Minoux, and Pierre Legagneux, *Appl. Phys. Lett.* Vol. **89**, (2006), p. 022111

[12] X.L. Han, G. Larrieu and E. Dubois, *J. Nanosci. Nanotechnol.* Vol. 10, (2010), p. 7423-7427

[13] Z.K.Chen, E. Dubois, F. Ravaux and F. Danneville, *Microelectronic Engineering*, Vol. 97, (2012), p. 280-284

[14] L. Hudanski, E.Minoux, L.Gangloff, K.B.K. Teo, J-P. Schnell, S. Xavier, J. Robertson, W.I. Milne, D. Pribat and P. Legagneux, *Nanotechnology*, Vol. 19, (2008), p. 105201.

Figure Captions

Figure 1 (Color online) Schematic representation of fabrication process of individual carbon nanotube array: (1) realization HSQ nanopillar on Ni surface, (2) Etching Ni layer by IBE, (3) Etching TiN layer by RIE, (4) Stripping of HSQ resist, (5) Growth individual CNT.

Figure 2 (Color online) Cross-section views of high resolution of SEM image showing bi-layer Ni and TiN deposited on Si substrate.

Figure 3 (Color online) Left: SEM image of HSQ resist pattern arrays (Pitch = 5 µm) with high contrast value on Ni surface after e-beam exposure and development by 25% TMAH. Right: zoom SEM image of HSQ nanopillar (Φ = 134 nm; and H = 82 nm).

Figure 4 (Color online) (a) SEM image of nano dot after etching Ni by IBE, (b) after etching TiN by RIE, (c) SEM images of the nano dots arrays after stripping the HSQ resist patterns by Pedatch solution, (d) zoom SEM image of nanodot Ni/TiN (Inset: SEM image 30° tilt, scale bar is 50 nm).

Figure 5 (Color online) Left: SEM image of single carbon nanotube grown on TiN-Si nano dots array with 20 µm pitch, deposited by PECVD for 10 min; Right: Zoom SEM image of CNT with high aspect ratio ‘‘whisker-like’’ shape produced on TiN-Si nanodot.

Figure 6 (Color online) Left: Schematics of measurement system in the experiment; Rigth: the field emission measurement of individual vertical carbon nanotube array, the maximum current of 4.23 mA for an applied electric field of 22.5V/µm.

Growth of individual carbon nanotubes on an array of TiN/Ni nanodots patterned by e-beam lithography and defined by dry etching for field emission application.

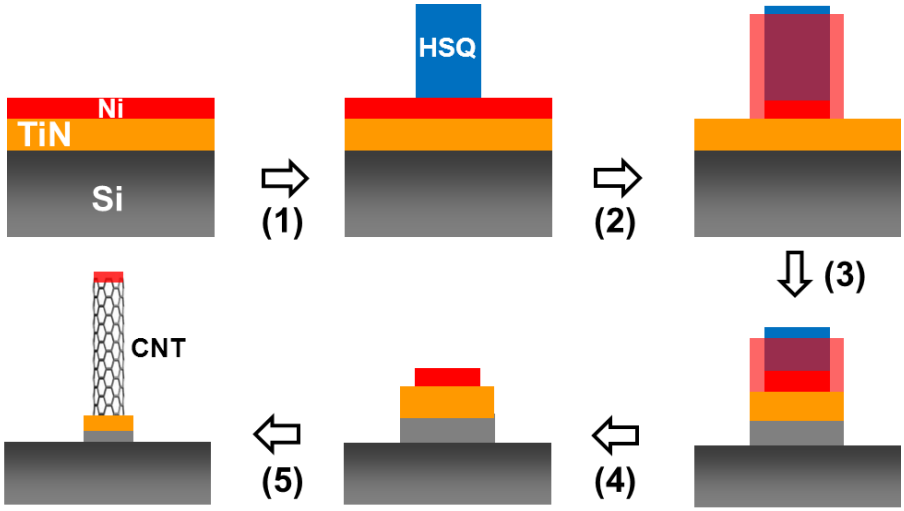


Figure 1

Growth of individual carbon nanotubes on an array of TiN/Ni nanodots patterned by e-beam lithography and defined by dry etching for field emission application.

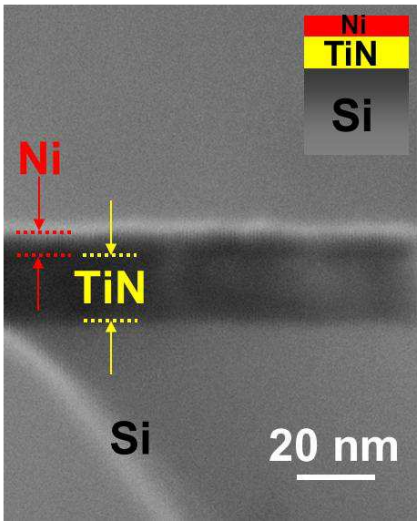


Figure 2

Growth of individual carbon nanotubes on an array of TiN/Ni nanodots patterned by e-beam lithography and defined by dry etching for field emission application.

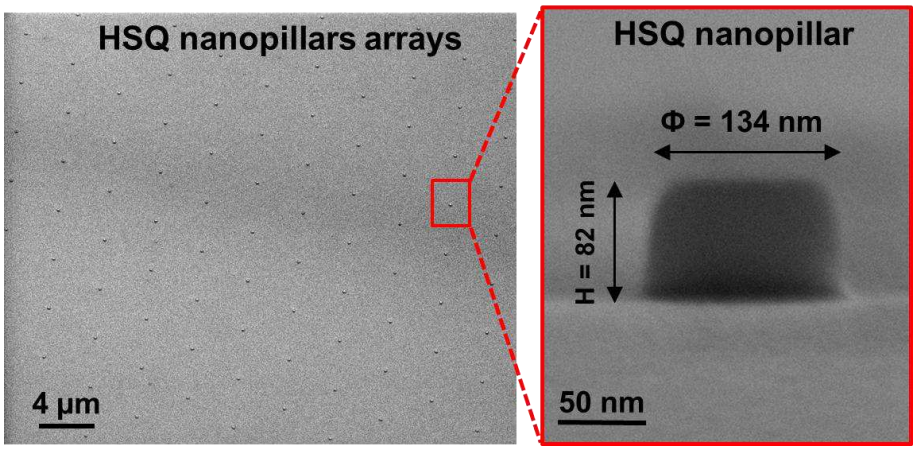


Figure 3

Growth of individual carbon nanotubes on an array of TiN/Ni nanodots patterned by e-beam lithography and defined by dry etching for field emission application.

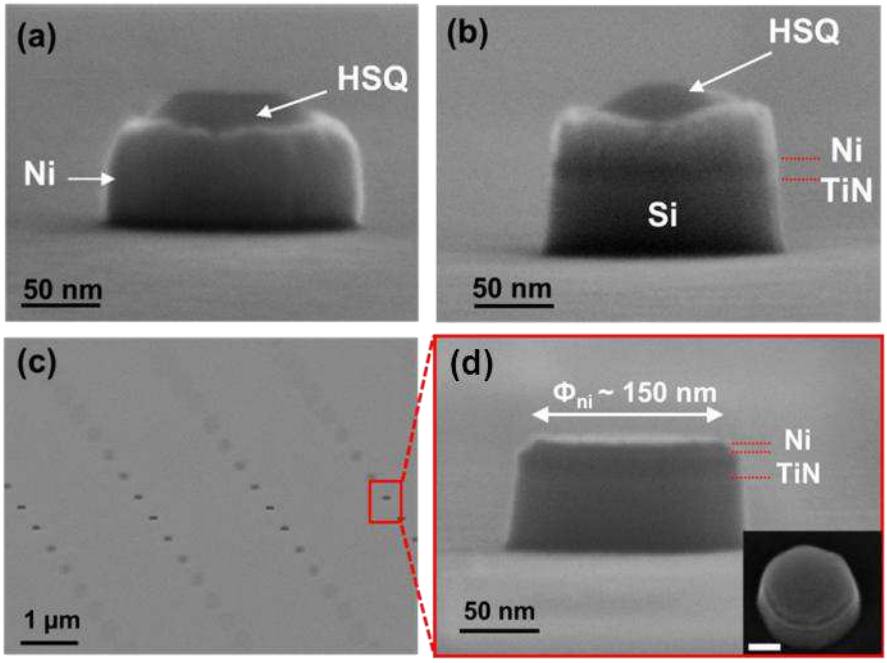


Figure 4

Growth of individual carbon nanotubes on an array of TiN/Ni nanodots patterned by e-beam lithography and defined by dry etching for field emission application.

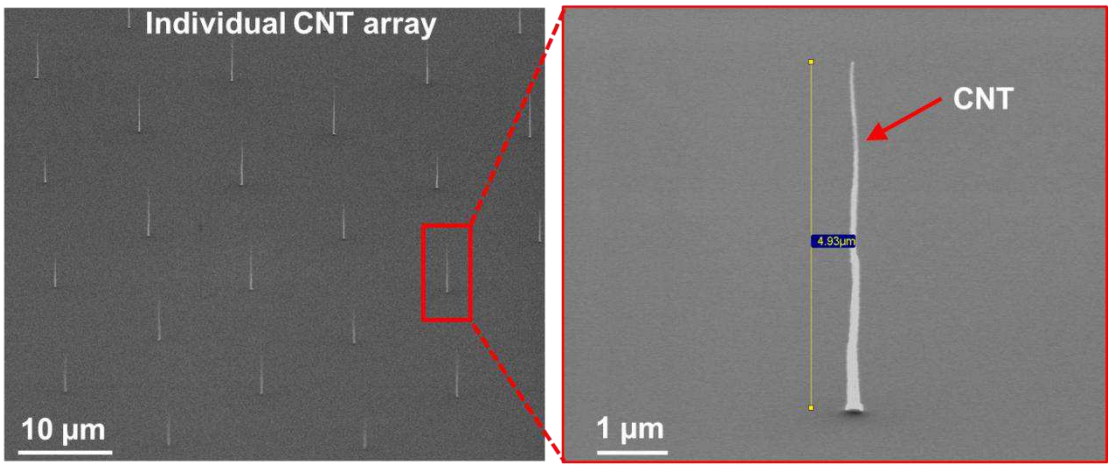


Figure 5

Growth of individual carbon nanotubes on an array of TiN/Ni nanodots patterned by e-beam lithography and defined by dry etching for field emission application.

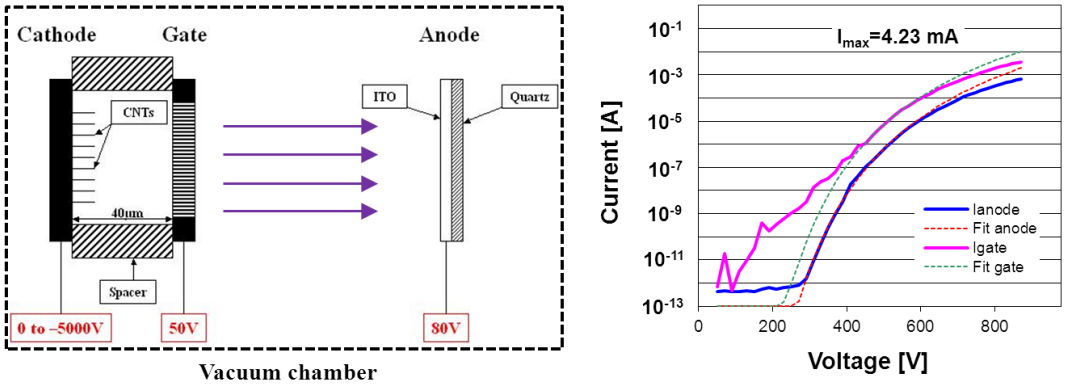


Figure 6